CLM-R282

CLM-R282

Large scale mixing calculations

D. F. Fletcher

UK ATOMIC ENERGY AUTHORITY

Culham Laboratory

CLM-R282

Large scale mixing calculations

D. F. Fletcher

Culham Laboratory, Abingdon, Oxon, OX14 3DB, UK

Abstract

The coarse mixing stage of a vapour explosion has attracted a considerable amount of interest in the study of hypothetical reactor accidents. Numerous models of this process have been developed. This paper contains a description of some large scale coarse mixing calculations and the results obtained using the CHYMES computer code. Exactly the same calculations are being performed by Prof. Theofanous and Prof. Bankoff using their own models. The aim of this work is to compare the results obtained from each of the codes and to examine the validity of the different assumptions made in the different models.

Culham Laboratory
United Kingdom Atomic Energy Authority
Abingdon
Oxfordshire OX14 3DB

January 1988

ISBN: 085311 1677
C/18 Price: £4.00
Available from H.M. Stationery Office

Contents

		Page No.
1.	Introduction	1
2.	Description of the Calculation	1
3.	Modifications to CHYMES	2
4.	Results of the Computations	3
	4.1 Hydrodynamics Results for Case 1	3
	4.2 Mixing Results for Case 1	5
	4.3 Results for Case 2	7
	4.4 The Effect of Ambient Pressure	7
5.	Discussion	9
	Acknowledgements	10
	References	11
	Figures	

1. Introduction

Developing an understanding of the mixing stage of a vapour explosion is of considerable interest in the study of hypothetical reactor accidents. Numerous models of coarse mixing have been produced and are reviewed in reference 1. Since that review was produced Theofanous and co-workers [2] have produced a model similar to that developed by Bankoff and co-workers [3]. In addition, a new model has been developed at Culham based on the recommendations made in the review. This model is transient, two-dimensional and allows for slip between all phases. It is fully described in references 4 and 5.

In this paper we present the results of some large scale simulations using the Culham code (named CHYMES). Some of these simulations are being carried out by both Prof. Theofanous and Prof. Bankoff so that the different models can be compared.

The paper is organised as follows: section 2 contains a description of the geometry and conditions used in the calculations; section 3 contains a brief description of the changes made to the CHYMES code to enable the calculation to be performed; section 4 contains the computational results and section 5 contains a discussion.

2. Description of the Calculation

The geometry chosen for the comparison exercise is shown in Figure 1. The annular steps removed from the cylindrical vessel are a first attempt at representing a hemispherical base.

The vessel was 4.4 m in diameter and 2 m high and was initially filled with saturated water at a pressure of 0.1 MPa, consisting of 95% liquid water and 5% steam. Melt was injected vertically downwards with a speed of 2m/s over a 1 m radius region with a volume fraction of 0.5 throughout the duration of the simulation. This inflow condition models

melt pouring through holes in a plate, so that whilst melt flows in, water and steam cannot flow out. The remainder of the vessel top was closed, except for a small annular exit. The melt was assumed to have a density of 7.5×10^3 kg/m^3 and its temperature and particle size were held fixed at 2500 K and 20 mm, respectively. (The options in the code to evolve the melt temperature and the melt and water length-scales were switched off.)

The vessel was modelled using a finite difference grid consisting of 11 cells in the radial direction and 10 cells in the vertical direction. A time-step of 2×10^{-5} s was used. The constitutive relations used took the form given in references 1 and 2. The steam and water length-scales were set to a constant value of 20 mm.

The usual boundary conditions were used on the solid walls, i.e. the normal velocity component was set to zero. The outlet boundary condition had to be modified as in all previous work we assumed that the flow at the outlet was developed (as the exit was a long way from the mixing region). The obvious choice of boundary condition for the present simulation was one of constant pressure. The changes made to the code to allow this to be implemented are given in the next section.

3. Modifications to CHYMES

The calculations involved two new features not used before. These were the removal of the annular steps from the solution domain and the implementation of a constant pressure boundary condition.

The first of these, the removal of annular regions from the solution domain, was very easily achieved by ensuring that the steps were located at finite difference cell boundaries. Then vertical walls were modelled by setting $V = 0$ and horizontal walls were modelled by setting $U = 0$, ensuring that the normal component of the velocity was zero at all solid boundaries. A geometry array (called IGEOM) has been added to the coding to enable any user-specified regions to be treated as solid regions.

The second change, the implementation of a constant pressure boundary condition, was more complicated. The pressure was set to a constant value upstream of the last solved V-velocity nodes in the outlet region. The code was then modified so that one more pressure and one more velocity were solved in each vertical sweep. Care was needed to ensure that values of, for example, volume fractions at the last cell exit were suitably defined. Once the correct procedure had been developed the constant pressure boundary condition was found to give good results, i.e. continuity errors were always low in the exit region and the flow was always outwards, as expected.

4. Results of the Computations

In this section we will present a selection of the results available from the output of the code. The first case, with the larger vent width of 0.4 m, will be described in detail. The second case, with a vent width of 0.2 m will then be compared with the first case. In addition, we briefly describe the results of two further computations, carried out to examine the effect of ambient pressure on mixing.

4.1 Hydrodynamics Results for Case 1

Figures 2(a), (b), (c), 3(a), (b), (c) and 4(a), (b), (c) show volume fraction contours of steam, water and melt at times of 0.2s, 0.5s and 1.0s after the start of the simulation. At 0.2s melt has penetrated about a third of the vessel depth and water has been removed from the region where melt is being injected. A very high volume fraction of steam ($\sim$ 80%) exists around the sides of the melt.

At 0.5s the pattern is similar except that melt has penetrated about three-quarters of the way to the base of the vessel. There is much more steam present. Most of the water is located in the base of the vessel or around the vessel sides.

After 1.0s the picture is very different. A substantial amount of melt has reached the vessel base and melt has collected on the horizontal surfaces of the annular steps in the vessel. The water volume fraction is less than 40% everywhere and most of the water is located in regions over-lying melt. The steam volume fraction is greater than 60% throughout most of the solution domain.

Figures 5(a), (b), (c), 6(a), (b), (c) and 7(a), (b), (c) show flux plots for steam, water and melt at times of 0.2s, 0.5s and 1.0s, respectively. The flux is the product of the volume fraction and velocity of a given species. At 0.2s melt is moving downwards with little spreading, with water being pushed away and steam flowing through the melt and along the top wall to the exit. At the later times melt is swept towards the outlet. The water flux is only non-zero in regions close to the vessel walls and there is a large steam flux throughout the vessel.

The detailed output from the code shows that there are large differences between the speeds of the different species. The figures show that in some regions water and steam are flowing in different directions. At the exit typical speeds are 100 m/s for the steam, 10 m/s for the water and 5 m/s for the melt. The peak vapour velocity during the calculation was 110 m/s, which gives a Mach number of ~ 0.25 so that the assumption of incompressible flow is reasonable (i.e. the flow would not be choked at the outlet). The sound speed used was that for steam, as the steam volume fraction was close to unity at the exit. However, it is well-known that even a small volume fraction of water in a gas can reduce the sound speed significantly [9]. Thus the valididity of this assumption can only be verified by carrying out simulations with a compressible flow code.

Figure 8 shows the cumulative mass of melt and water swept-out of the vessel as a function of time. The figure shows that for the first 0.8s water was expelled at an approximately constant rate of 16 tonnes per second and for the final 1.2s of the calculation there was very little sweep-out. The initial phase of sweep-out corresponds to the time when the melt front has not yet reached the vessel base, during which stage melt and steam are pushing water aside which is expelled out of the vent.

Melt starts to be expelled after about 0.5s and about 1.5 tonnes of melt is expelled in the next second and then there is very little further sweep-out of melt.

Initially the vessel contained 18 tonnes of water so that approximately 90% of the water was expelled during the simulation. Melt was injected at a rate of 24 tonnes/second so that the melt loss was insignificant.

4.2 Mixing Results for Case 1

At present there is no means of determining precisely what constitutes an explosive mixture. Various workers have suggested different criteria for when melt can be considered to be sufficiently mixed. In this section we present results using two different methods.

A method developed by Prof. Theofanous is based on the notion that explosions will not occur if there is too much steam present. He chooses two different criteria (to reflect the uncertainty in our current knowledge) which are to assume that melt in a region where the coolant void fraction is less than a critical value is sufficiently mixed [2]. The coolant void fraction is the steam volume fraction divided by the sum of the steam and water volume fractions. He uses void fraction values of 70% and 90% in his work. Figure 9 shows the mass of melt where the void fraction is less than 70% and 90% as a function of time. The figure shows that the mass of melt mixed using the 90% and 70% void fraction limits are very high showing an almost continual increase with time to values of 40 and 35 tonnes after about 2 seconds. This method is somewhat misleading as it does not check explicitly how much water is present in the mixture zone.

An alternative criteria has been developed by Fletcher and Thyagaraja [6]. This uses a function θ which takes values between zero and one and consists of a function of the volume fractions and other variables which is maximised when there is an equal volume of melt and liquid water present in a mixture. The value of θ falls as one component becomes lean or if there is too much steam present or the melt particle

size is too large. Since, in the present work, a fixed particle size of 20 mm has been used, the critical particle size in the θ function was set to 20 mm. Thus θ was a function of the volume fractions only and no allowance for the effect of particle size was made.

Figure 10 shows the fraction of the vessel for which θ is greater than θ_m as a function of time for various values of θ_m. Depending on the choice of value for θ_m (which is varied between 0.2 and 0.6 in figure 10), the maximum fraction of the vessel filled with mixture varies between 50% and 20%. For $\theta_m = 0.2$ or 0.4 the volume of mixture increases until approximately 0.8s at which time the melt front reaches the vessel base and the mixing is reduced. For the case of $\theta_m = 0.6$ there is very little mixture until after 0.8s and this mixture is located above horizontal surfaces.

These results are best understood by examining the θ distribution throughout the vessel during various phases of the simulation. Figures 11(a), (b) and (c) show θ contours at times of 0.2s, 0.5s and 1.0s. At 0.2s there is mixing at the leading edge of the melt jet which has penetrated about one-third of the way through the water pool. At 0.5s the melt has been spread throughout a large part of the vessel. At 1.0s melt has accumulated on all the horizontal surfaces leading to 'islands' of mixture on the steps and an extended region of mixture on the vessel base.

Clearly one must remember that the finite difference grid is very coarse and that the horizontal steps are a computational convenience. However, during the fall phase there is considerable mixing unlike in other large-scale simulations carried out by the author [6]. The difference in this case is that there is a lid on the top of most of the vessel so that there is much less sweep-out of melt and water. We will return to this point in the discussion.

4.3 Results for Case 2

A second simulation was carried out with the vent width reduced to 0.2 m. The results obtained from this simulation were very similar to those obtained from the first simulation. In the bulk of the solution domain there was very little change in any of the computed properties. There were changes in the region of the exit with the peak vapour velocity increased to 192 m/s from 110 m/s in the first case. This gives a peak Mach number of 0.4 so that the assumption of incompressible flow is still reasonable.

4.4 The Effect of Ambient Pressure

Two further simulations were carried out, with the large vent geometry, for ambient pressures of 6 MPa and 15 MPa respectively. These will be referred to as Case 3 and Case 4. The aim was to investigate the effect of pressure on mixing. Earlier one-dimensional simulations [8] showed an important effect of pressure on mixing. At low pressure (0.1 MPa) large volumes of steam were produced which expelled liquid water and melt from the vessel. At intermediate pressures (6 MPa) the vapour flow rates were reduced and mixing was improved. At high pressure (15 MPa) the vapour flow rate was much lower and melt and coolant were found to separate out quickly as the stirring effect of the steam was reduced.

The present simulations suggest that this effect also occurs in the two-dimensional simulations carried out here. Table 1 below shows the cumulative mass of melt and water expelled at the end of the simulations as a function of pressure.

P (MPa)	Mass of melt expelled (t)	Initial Mass of water in vessel (t)	Mass of water expelled (t)	
0.1	1.4	18.0	16.2	(90%)
6.0	0.33	14.2	10.9	(75%)
15.0	0.27	11.3	8.1	(71%)

Table 1 : The effect of pressure on sweep-out

In all cases the mass of melt lost is insignificant. The mass of water lost falls with increasing pressure with a 90% loss at 0.1 MPa being reduced to 71% at 15 MPa. In all cases most of this loss occurred in the first second of the simulation. If there was no vapour production 30% of the water would have had to be expelled to accommodate the melt injected. Thus the results show that a large fraction of the water was dragged out of the vessel by the flow of steam.

Figures 12 and 13 show that fraction of the vessel filled with mixture for the simulations corresponding to pressures of 6 MPa and 15 MPa respectively. Comparison with figure 10 shows that mixing is improved during the first second for the case of a pressure of 6 MPa. Increasing the pressure further decreases the amount of mixing. (This effect is best observed by studying the $\theta_m = 0.6$ line.) At later times (after 1s) the amount of mixture decreases monotonically with increasing pressure. However, this stage is of less interest because melt has collected on horizontal surfaces and a much finer computational mesh would be needed to study this mixing properly (if it was thought to be important).

Figures 14(a), (b), (c) and 15(a), (b), (c) show plots of θ at times of 0.2s, 0.5s and 1.0s for the cases 3 and 4. The plots clearly show better mixing at $t = 0.2s$ compared with that for a pressure of 0.1 MPa (Figure 11(a)). In addition, there is undoubtedly better mixing at $t = 0.5s$ for the 6 MPa case. At 1.0s the pictures are more difficult to

interpret but there are 'islands' of good mixture in all of the simulations.

5. Discussion

In this paper we have described the results of a large scale simulation of coarse mixing. The simulation was carried out using the CHYMES code which has previously been used to simulate mixing in open-tank geometries (see [4], [5], [6] and [7]). In these situations mixing was always limited by the early sweep-out of melt and water which was unrestricted apart from the region in which melt inflow was prescribed.

The present simulation is very different in that the vessel is closed at the top except for a small exit. In this case sweep-out is inhibited during the melt fall phase and the flow of steam aids mixing by dragging melt through the water pool as it escapes.

The present calculation could be criticised on a number of assumptions:

(i) Melt inflow is imposed and the steam generated during mixing cannot change the amount of melt inflow.

(ii) The representation of the hemispherical vessel base is very crude.

(iii) The melt is injected with a pre-fragmented size of 20 mm.

(iv) The simulation is two-dimensional when all real flows are three-dimensional.

However, the simulation shows a number of interesting features and in particular it highlights the importance of geometry. In a previous paper [7] the author has illustrated the sensitivity of the mixing process to the melt injection conditions. Thus one of the main conclusions from this

work must be the need to understand and correctly model the initial and boundary conditions as these play an extremely important role in determining how much mixing occurs.

Simulations have also been carried out to examine the effect of pressure on mixing. They show that increasing the pressure produces improved mixing at 6 MPa (compared to 0.1 MPa) and reduced mixing at 15 MPa (compared to 6 MPa). A pressure of 6 MPa corresponds to the peak critical heat flux for water [1] suggesting that this may correspond to the worst case. However, these conclusions are based only on qualitative observations. It is not clear that vapour inhibits detonation to the same extent at high pressure as low pressure since the vapour density is much higher. Thus without experimental results for this pressure range it is difficult to draw any firm conclusions.

In addition, some of these simulations are to be compared with the results of a similar simulation being carried out by Prof. Theofanous and Prof. Bankoff using their own models. This should allow us to determine the strengths and weaknesses of each model and to examine the sensitivity of the predictions to different physical assumptions.

Acknowledgements

The author would like to thank his colleague Dr. A. Thyagaraja for useful discussions during the course of this work and to thank Mrs. M. Jones for her rapid and accurate preparation of this manuscript. The author would also like to thank Mr. I. Cook and Dr. B. D. Turland, Culham Laboratory, for helpful comments on a draft of this paper.

References

1. D. F. Fletcher, A review of coarse mixing models. Culham Laboratory report: CLM-R251, (1985).

2. M. A. Abolfadl and T. G. Theofanous, An assessment of steam-explosion-induced containment failure. Part II: Premixing Limits. Nucl. Sci. Engng., 97, 282-295, (1987).

3. S. G. Bankoff and A. Hadid, The application of a user-friendly code to nuclear thermal hydraulic reactor safety problems. Paper presented at the Int. Nuclear Power Plant Thermal Hydraulics and Operations Meeting, Taipei, Taiwan, ROC, 22-24 October, 1984.

4. A. Thyagaraja and D. F. Fletcher, Buoyancy-driven, transient, two-dimensional thermo-hydrodynamics of a melt-water-steam mixture. Comput. Fluids, 16, 59-80, (1988).

5. D. F. Fletcher and A. Thyagaraja, Numerical simulation of two-dimensional transient multiphase mixing. Proc. 5th Int. Conf. on Numerical Methods in Thermal Problems, Montreal, Canada, 29 June - 3 July, 1987, V(2), 945-956, Pineridge, (1987).

6. D. F. Fletcher and A. Thyagaraja, A method of quantitively describing a multi-component mixture. PhysicoChem. Hydrodynam., 9, 621-631, (1987).

7. D. F. Fletcher and A. Thyagaraja, Mathematical modelling of steam explosions. Culham Laboratory report: CLM-P831, (1987).

8. D. F. Fletcher and A. Thyagaraja, Numercial simulation of one-dimensional multiphase mixing. Culham Laboratory report: CLM-P776, (1986).

9. I. P. Jones and A. V. Jones, The numerical solution of simple one-dimensional multiphase flows in shock tubes. Paper presented at 2nd Int. Conf. on Numerical Methods in Laminar and Turbulent Flo.., Venice, 13-16 July, (1981).

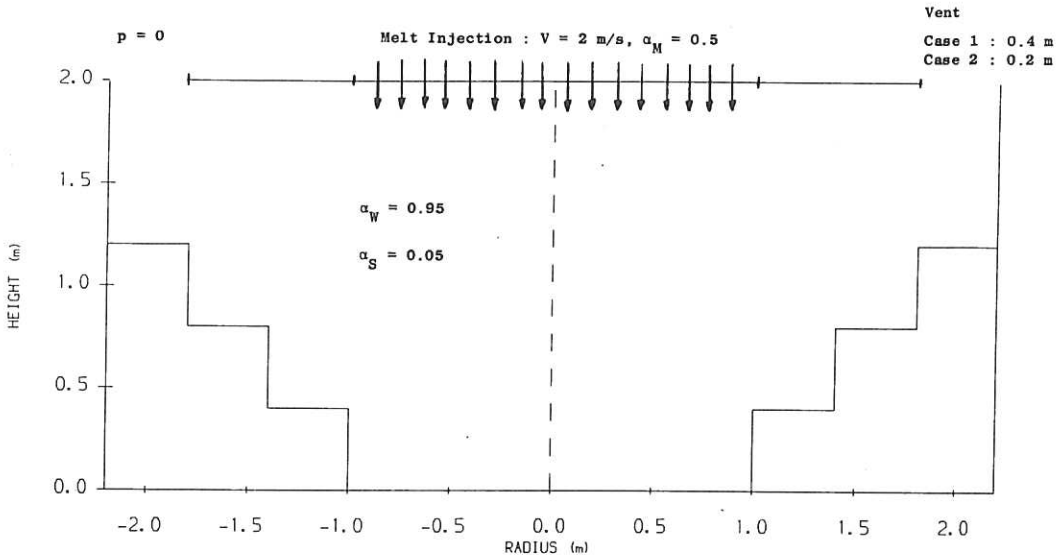

Fig.1: Geometry used in the simulation

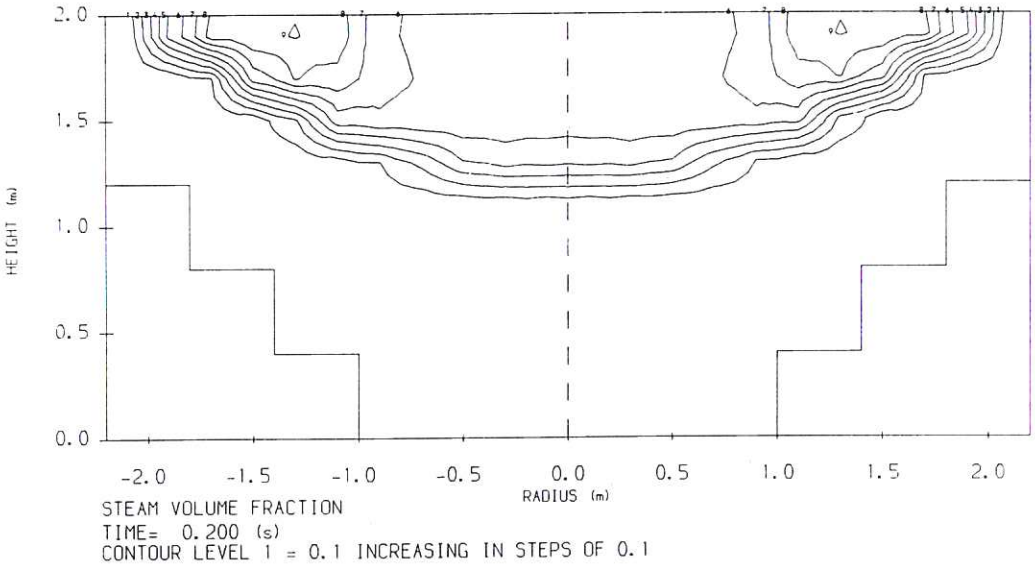

Fig.2(a): Steam volume fraction plot at t=0.2s.

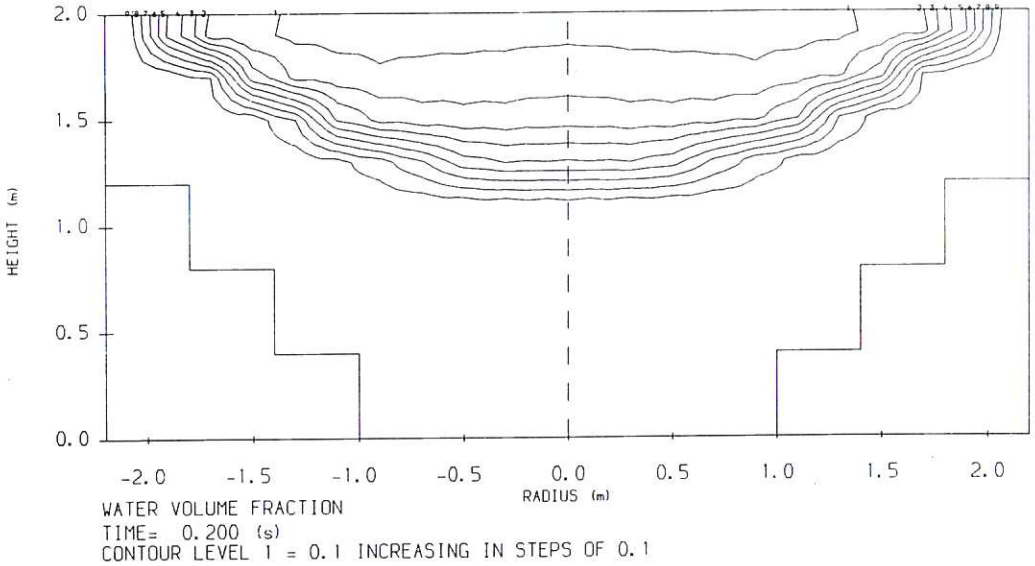

Fig.2(b): Water volume fraction plot at t=0.2s.

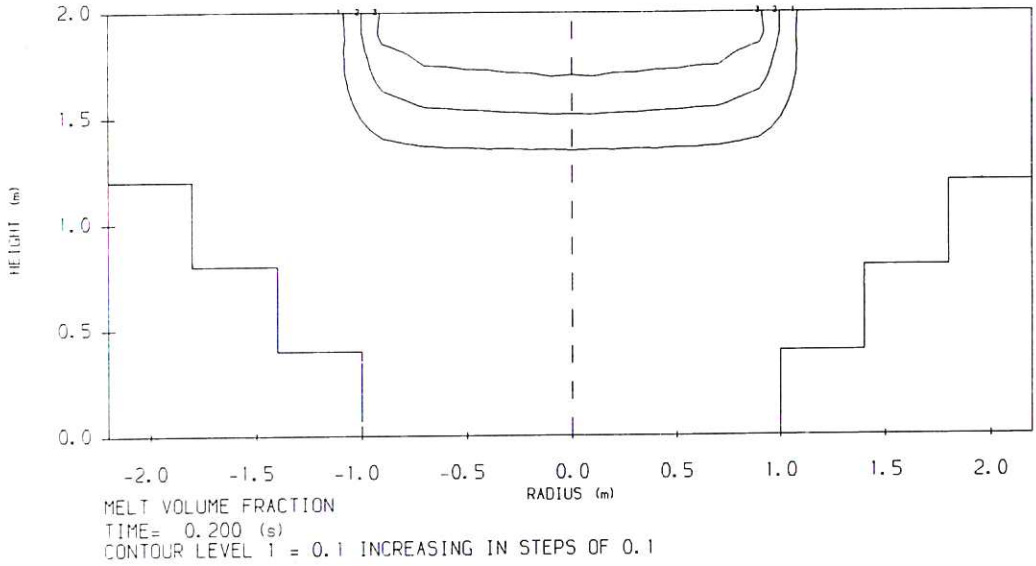

Fig.2(c): Melt volume fraction plot at t=0.2s.

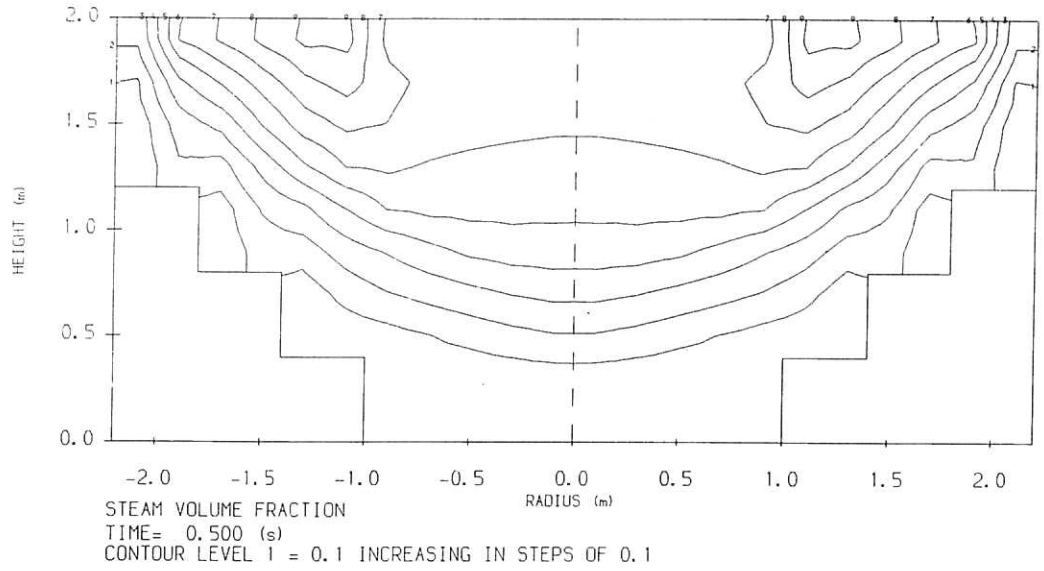

Fig.3(a): Steam volume fraction plot at t=0.5s.

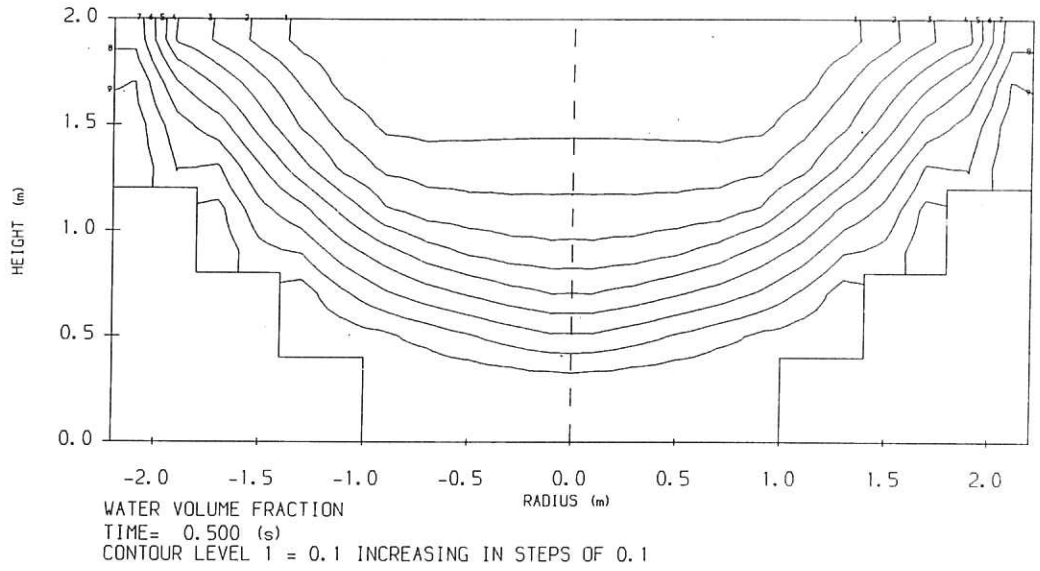

Fig.3(b): Water volume fraction plot at t=0.5s.

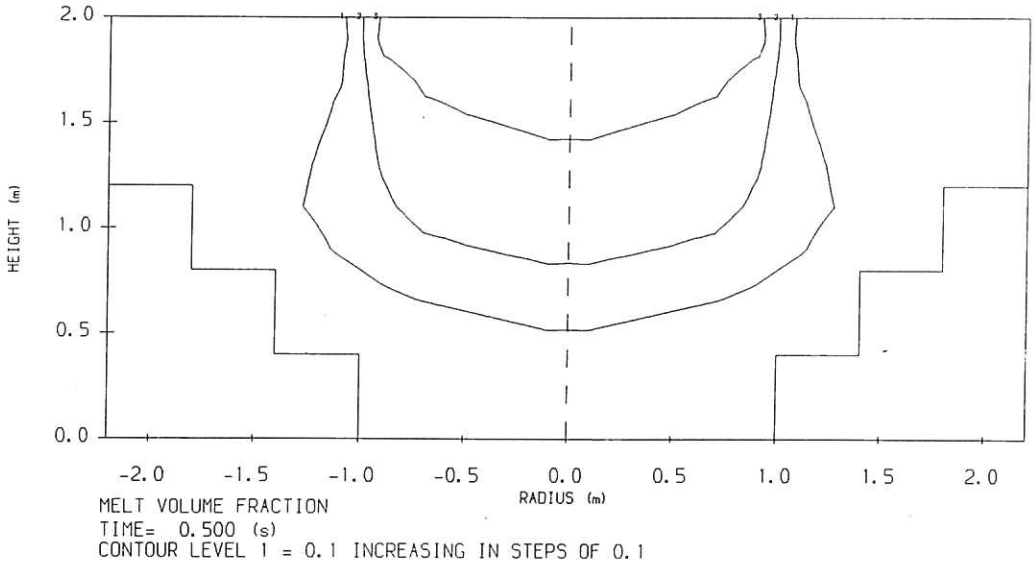

Fig.3(c): Melt volume fraction plot at t=0.5s.

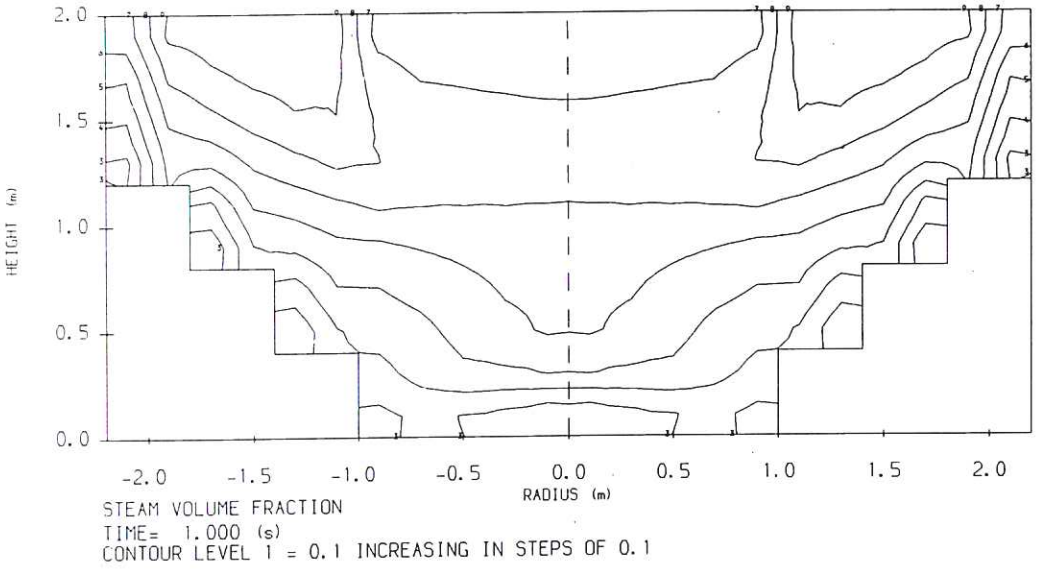

Fig.4(a): Steam volume fraction plot at t=1.0s.

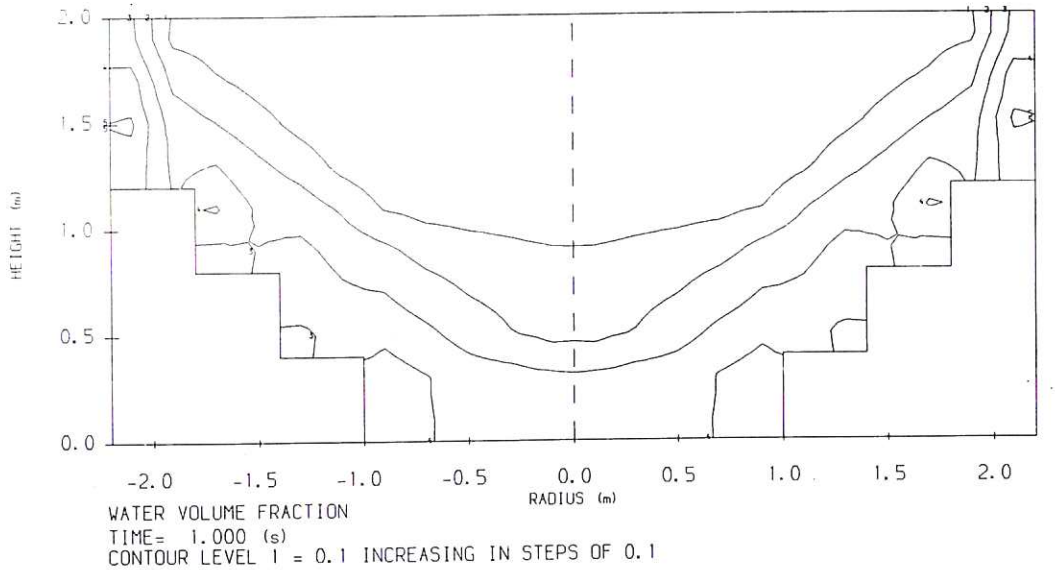

Fig.4(b): Water volume fraction plot at t=1.0s.

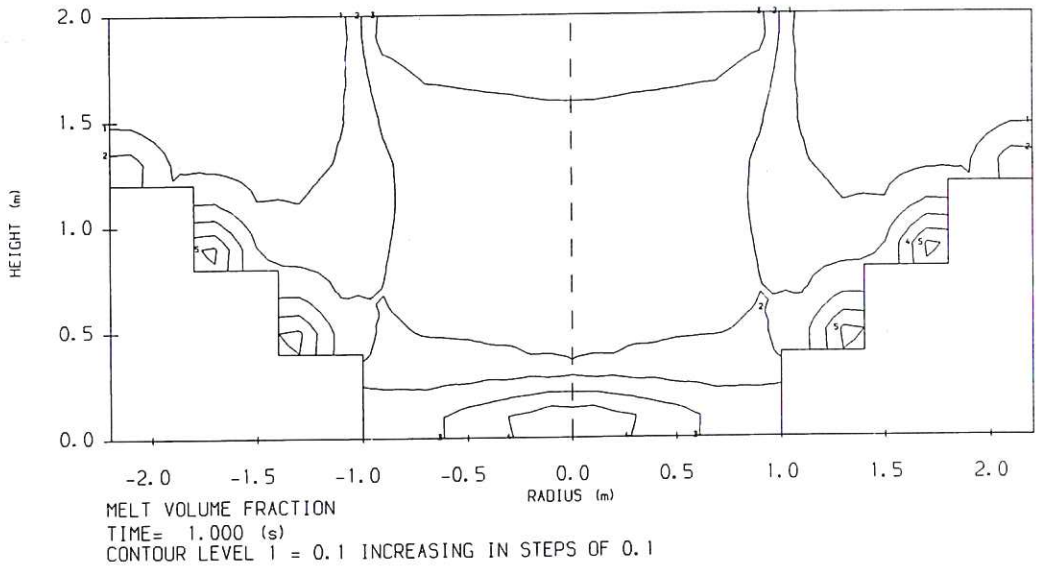

Fig.4(c): Melt volume fraction plot at t=1.0s.

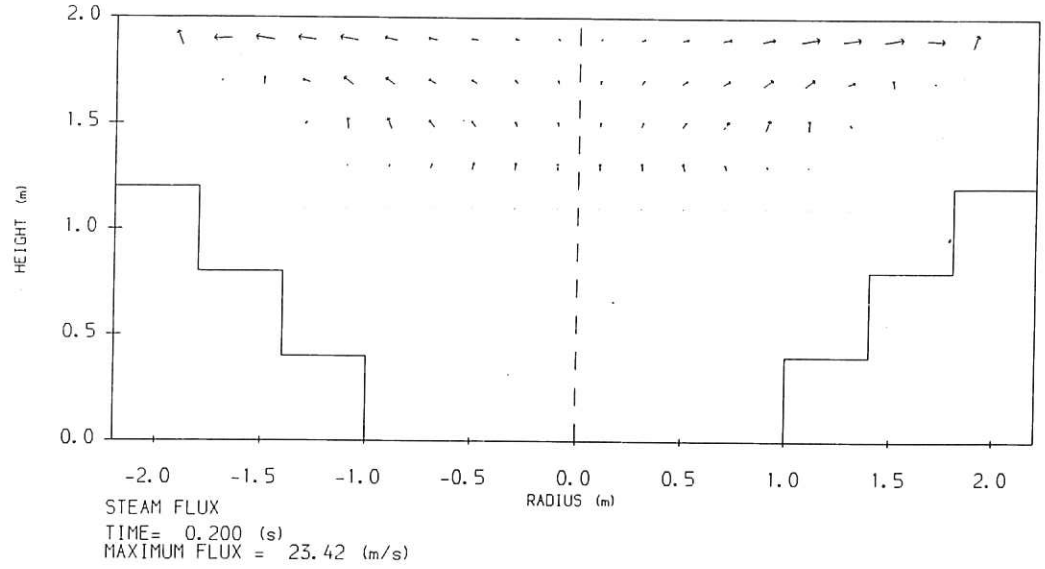

Fig.5(a): Steam flux plot at t=0.2s.

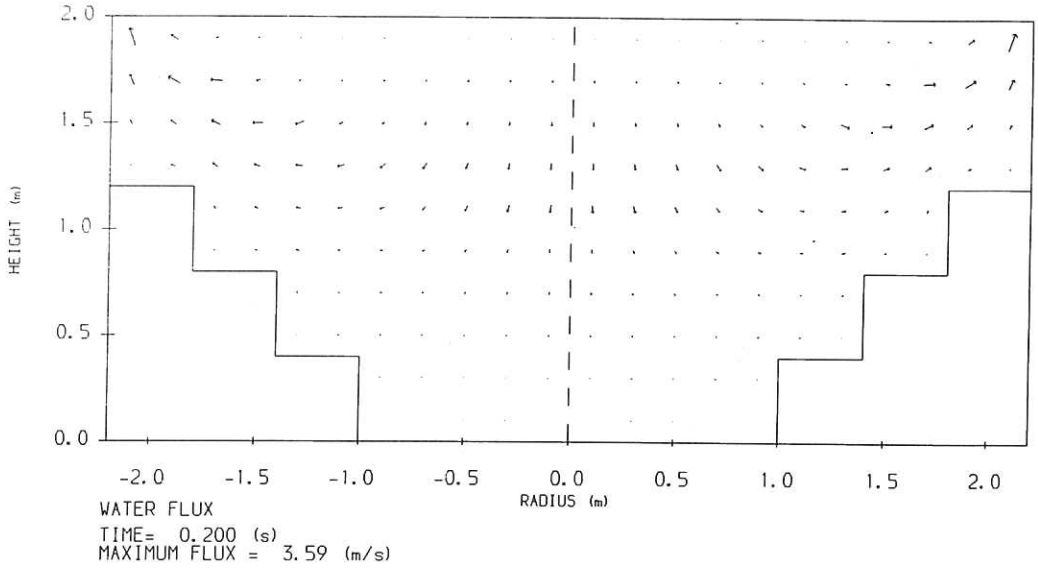

Fig.5(b): Water flux plot at t=0.2s.

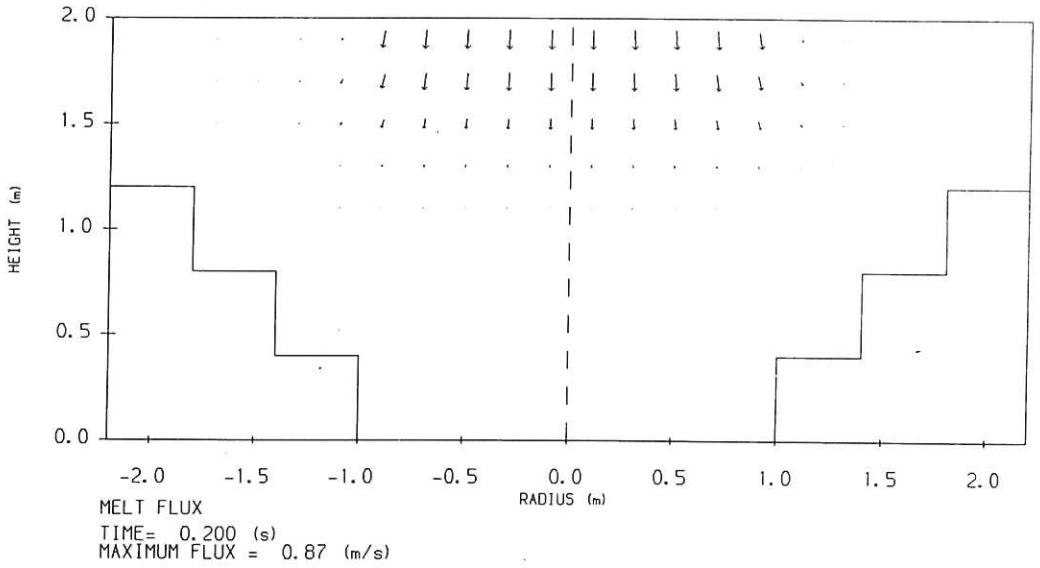

Fig.5(c): Melt flux plot at t=0.2s.

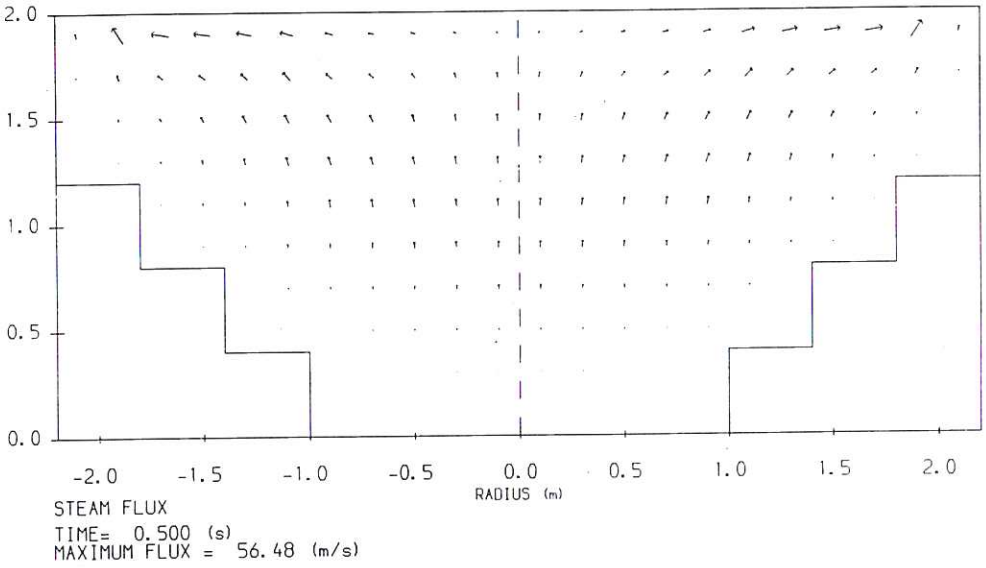

Fig.6(a): Steam flux plot at t=0.5s.

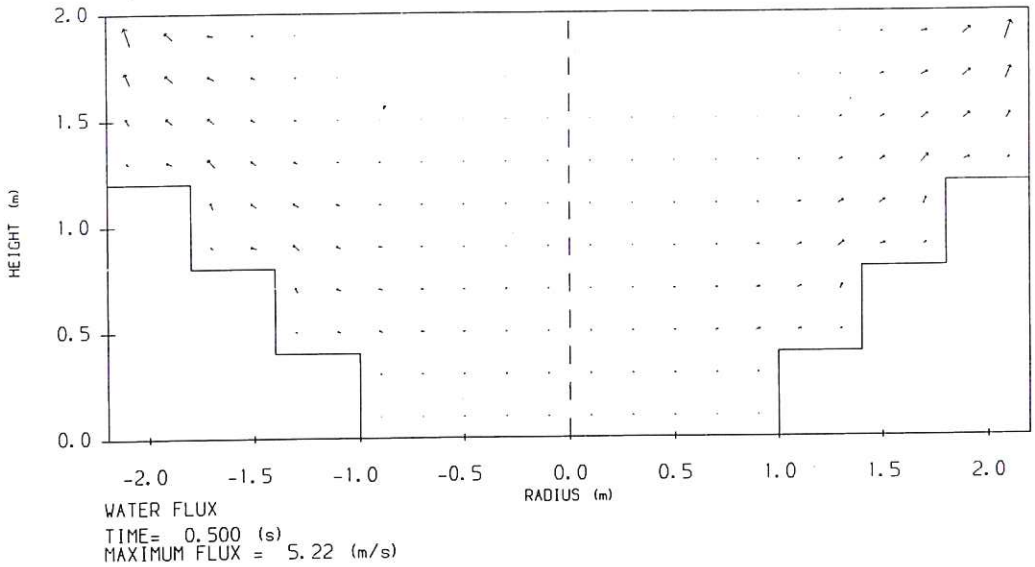

Fig.6(b): Water flux plot at t=0.5s.

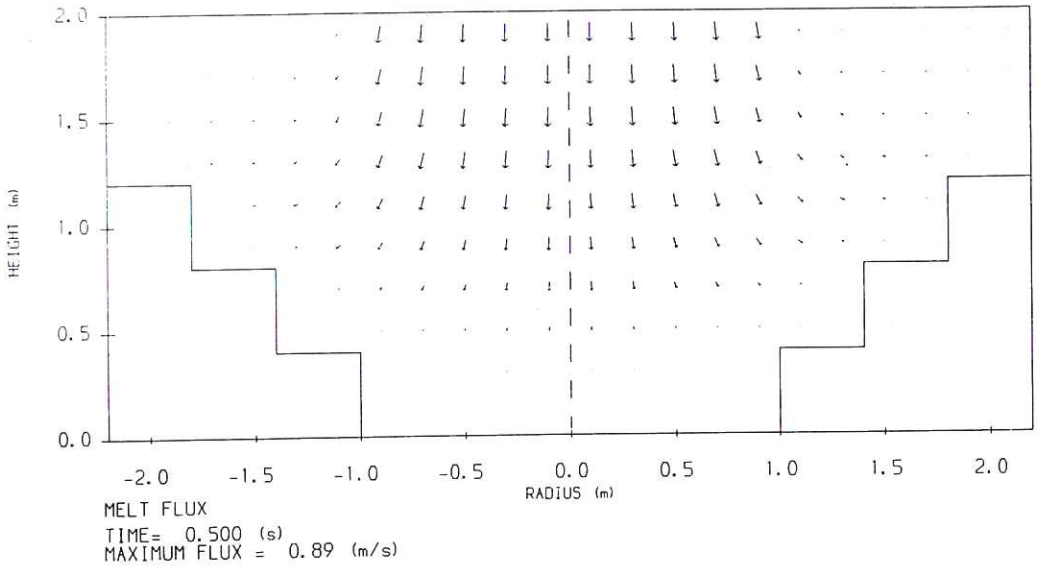

Fig.6(c): Melt flux plot at t=0.5s.

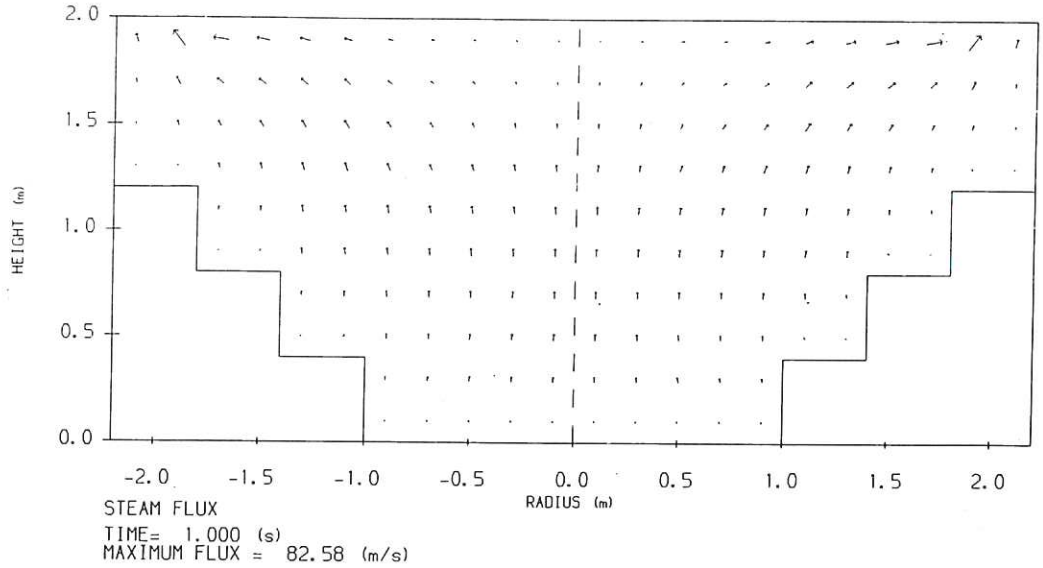

Fig.7(a): Steam flux plot at t=1.0s.

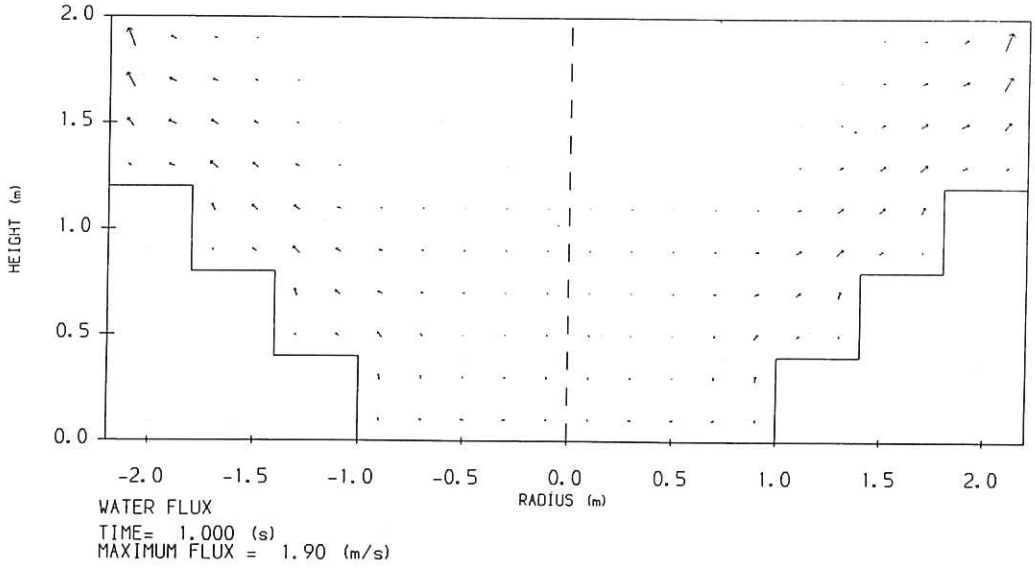

Fig.7(b): Water flux plot at t=1.0s.

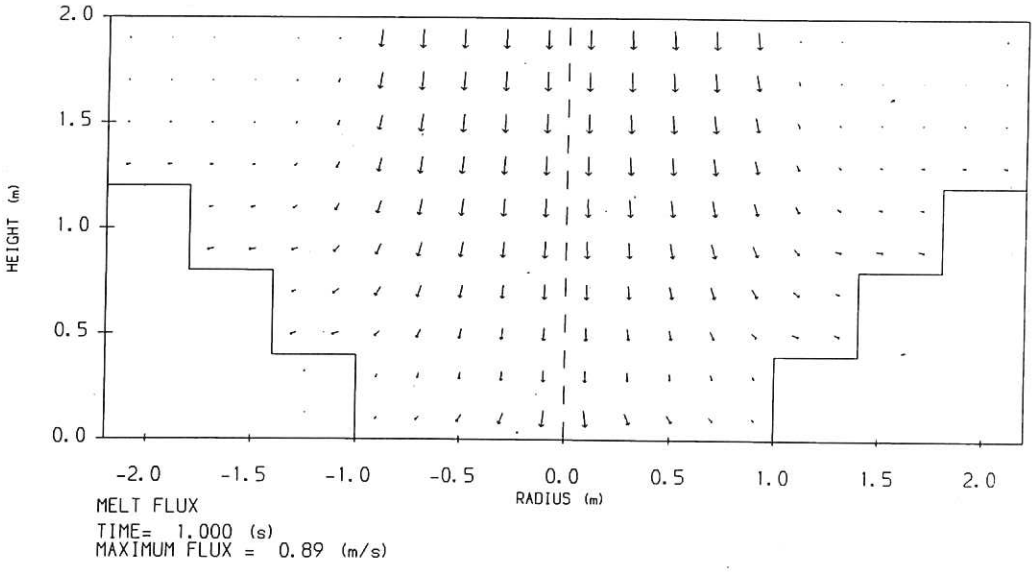

Fig.7(c): Melt flux plot at t=1.0s.

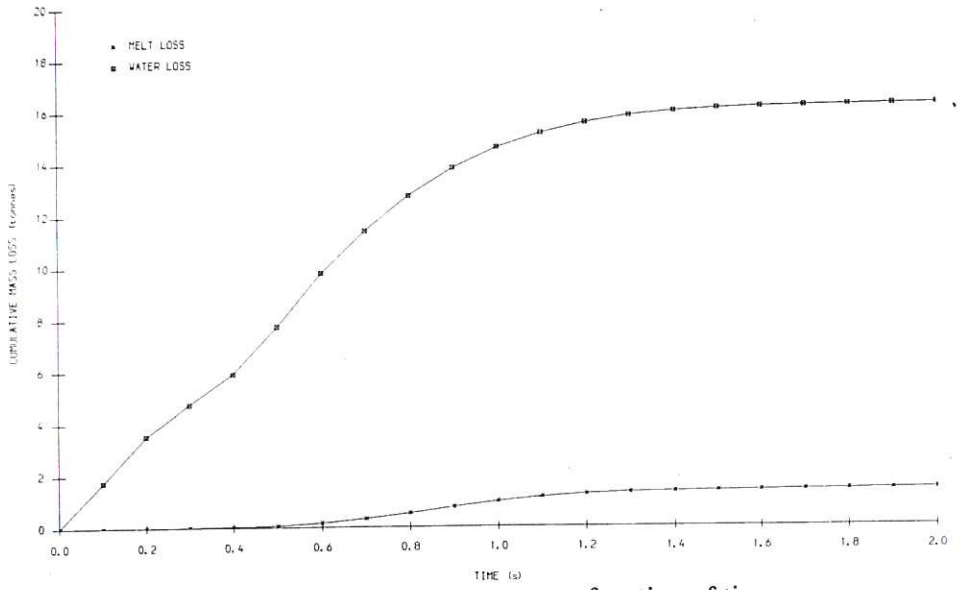

Fig.8: Melt and water sweep-out as a function of time.

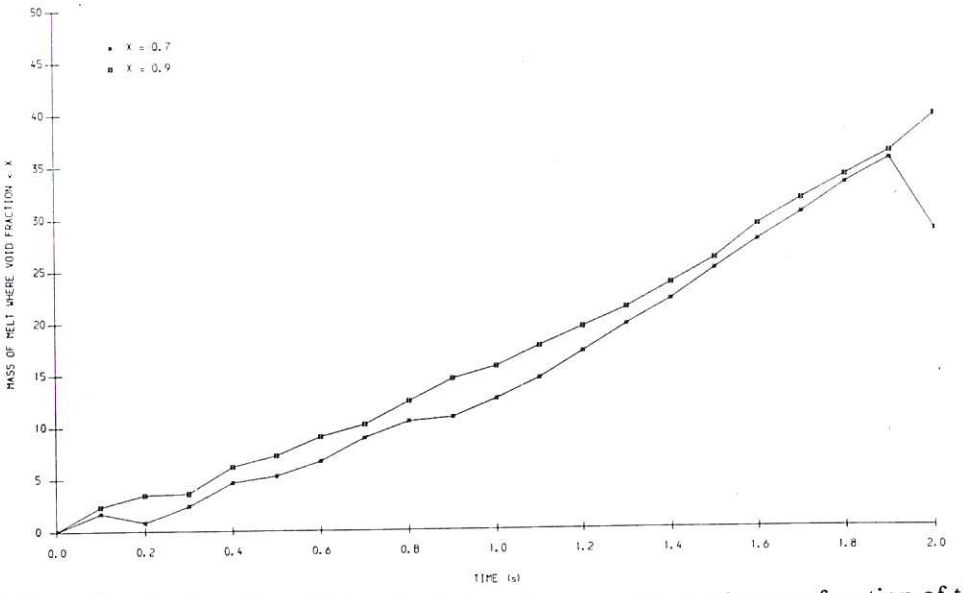

Fig.9: Mass of melt where the void fraction is less than a specified value as a function of time.

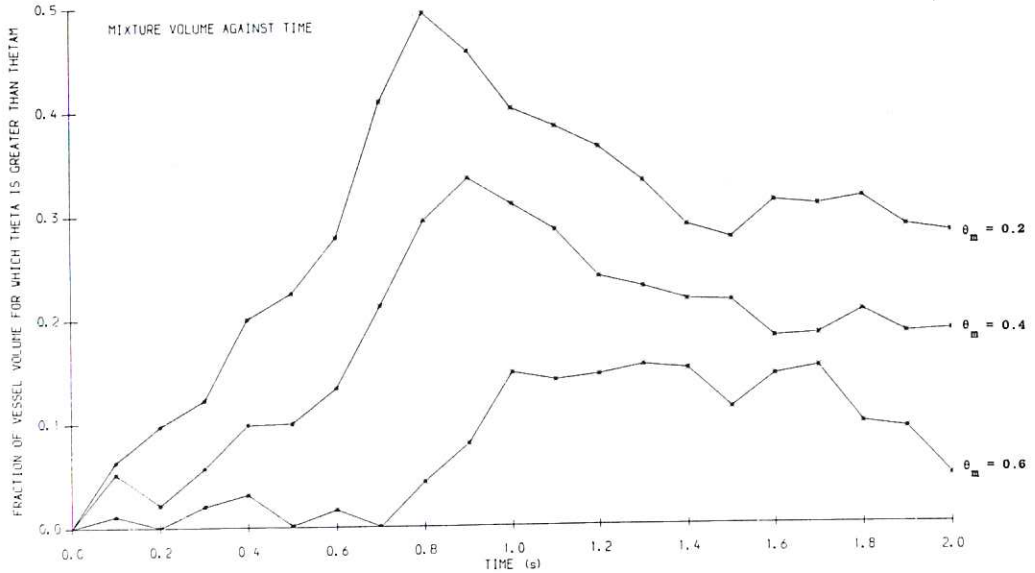

Fig.10: Fraction of vessel for which $\theta > \theta_m$ as a function of time.

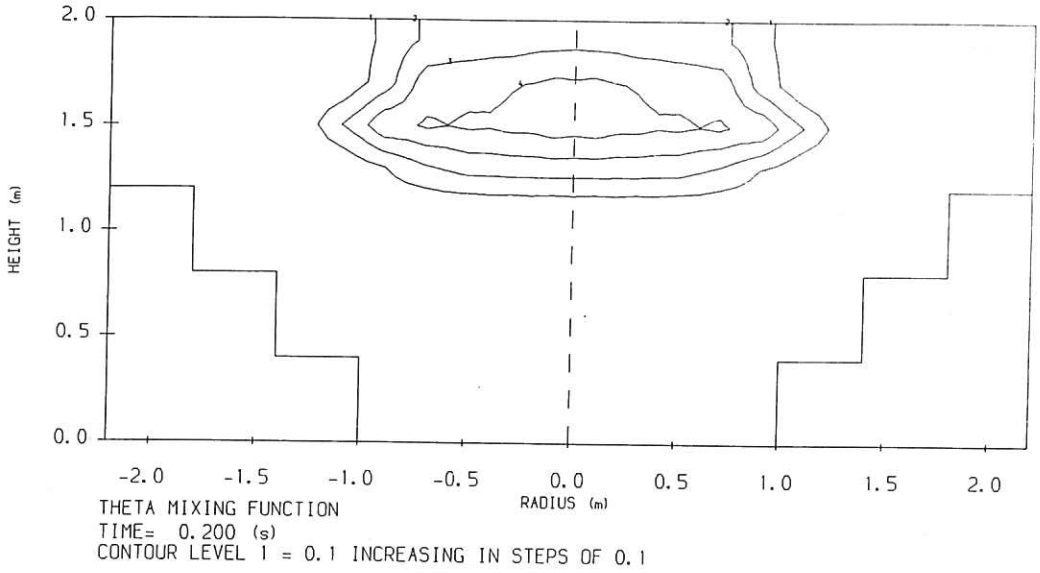

Fig.11(a): Theta function contours at t=0.2s.

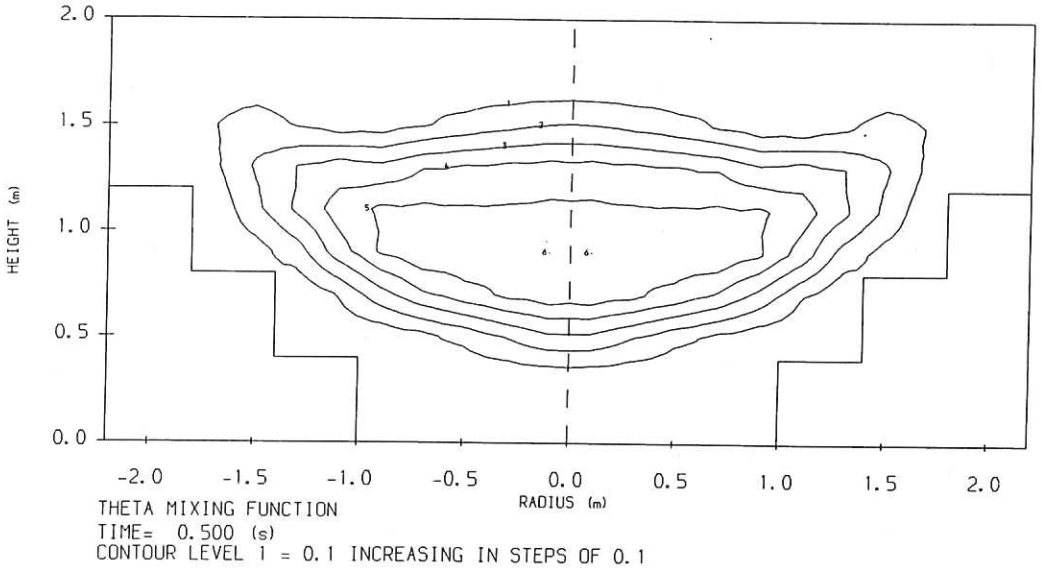

Fig.11(b): Theta function contours at t=0.5s.

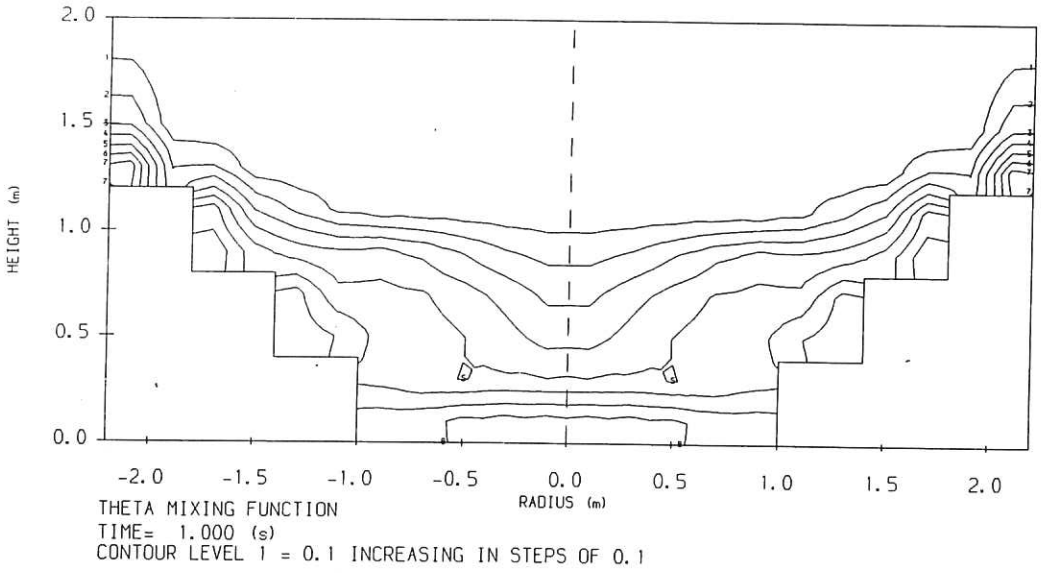

Fig.11(c): Theta function contours at t=1.0s.

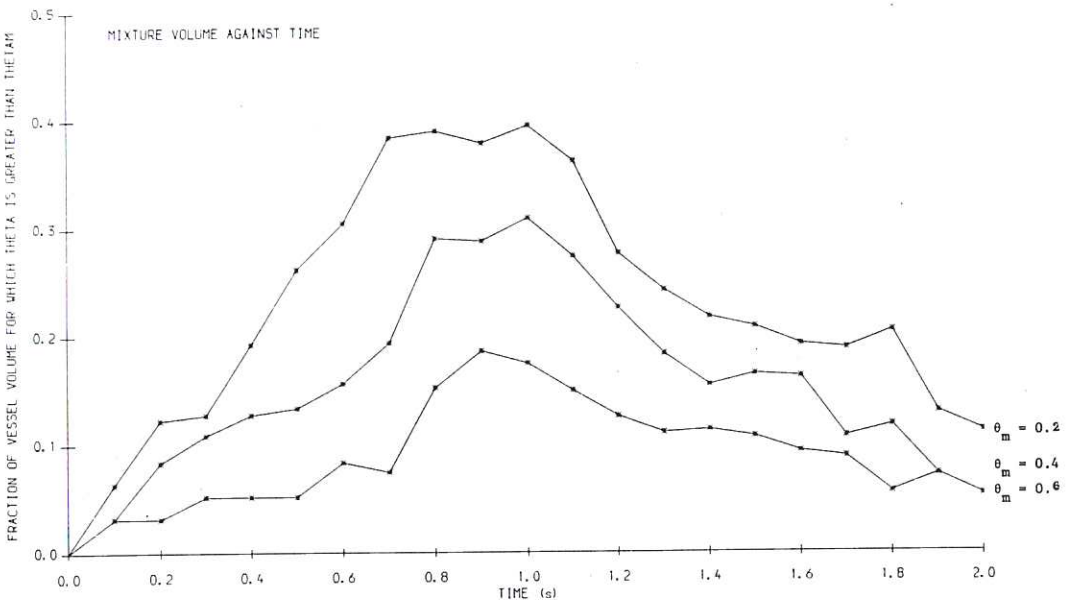

Fig.12: Fraction of vessel for which $\theta > \theta_m$ as a function of time for an ambient pressure of 6MPa.

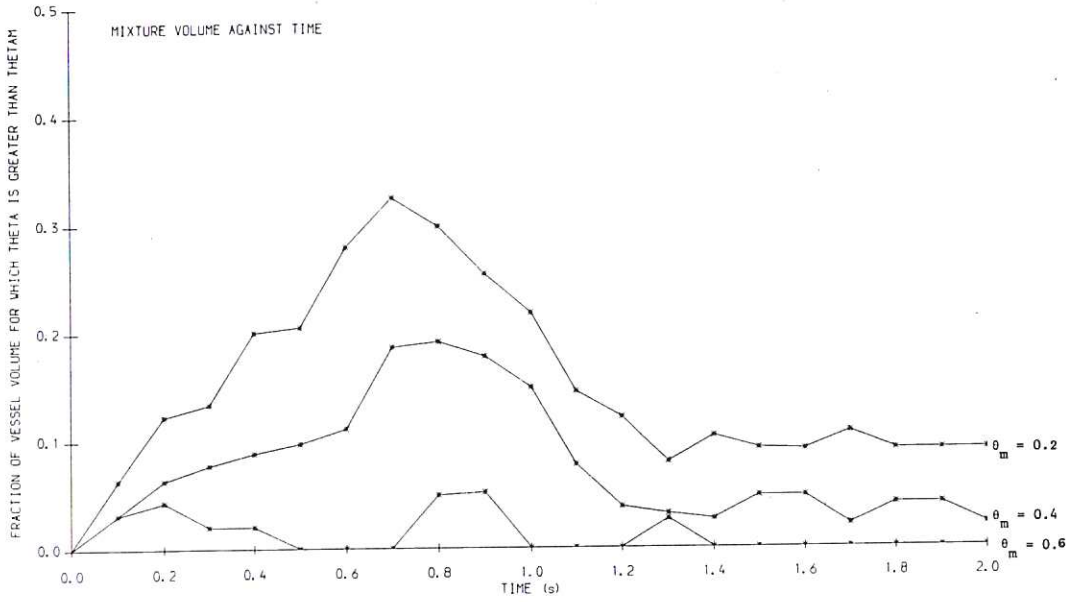

Fig.13: Fraction of vessel for which $\theta > \theta_m$ as a function of time for an ambient pressure of 15MPa.

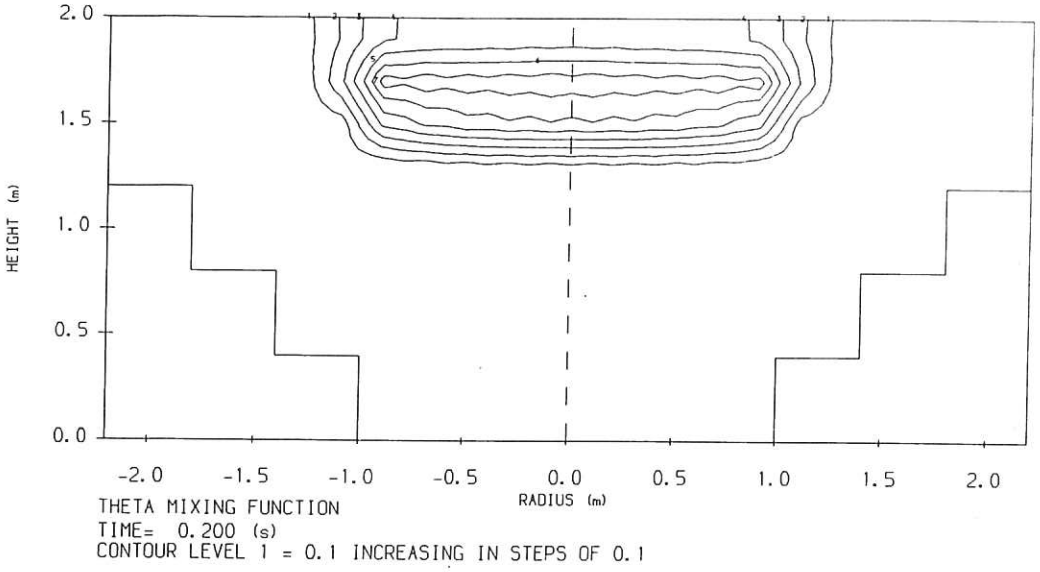

Fig.14(a): Theta function contours at t=0.2s for an ambient pressure of 6MPa.

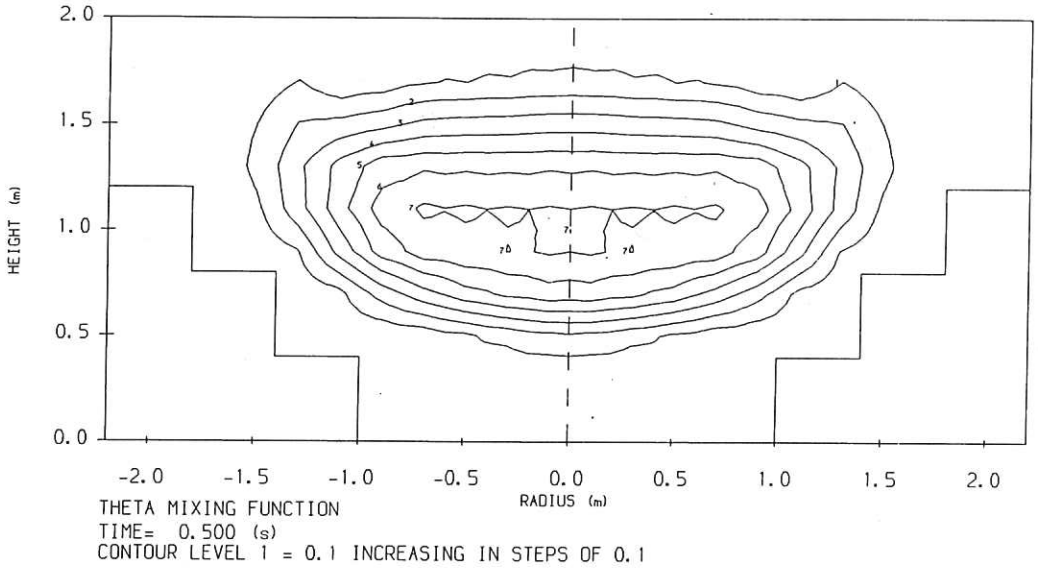

Fig.14(b): Theta function contours at t=0.5s for an ambient pressure of 6MPa.

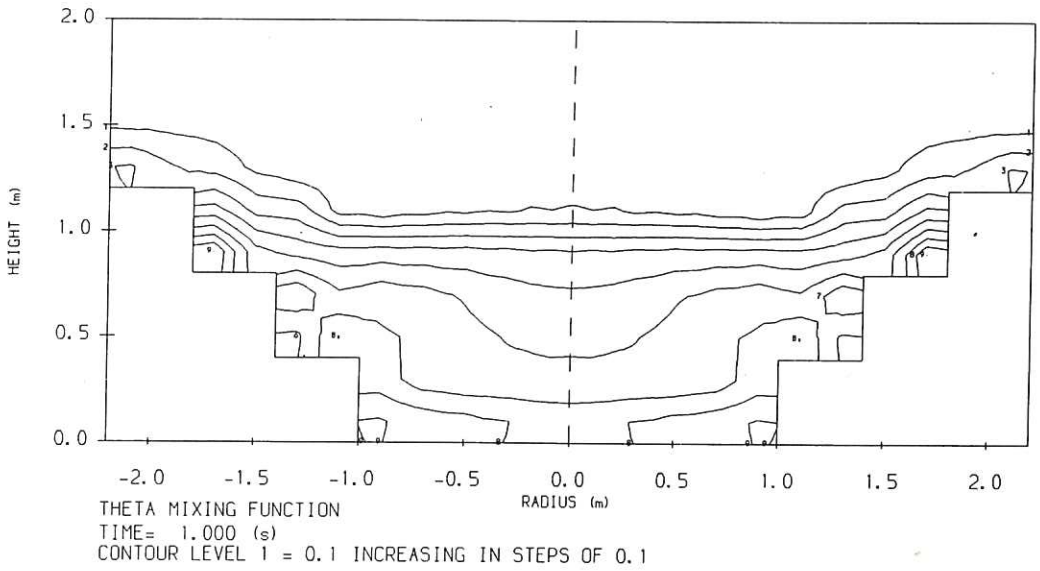

Fig.14(c): Theta function contours at t=1.0s for an ambient pressure of 6MPa.

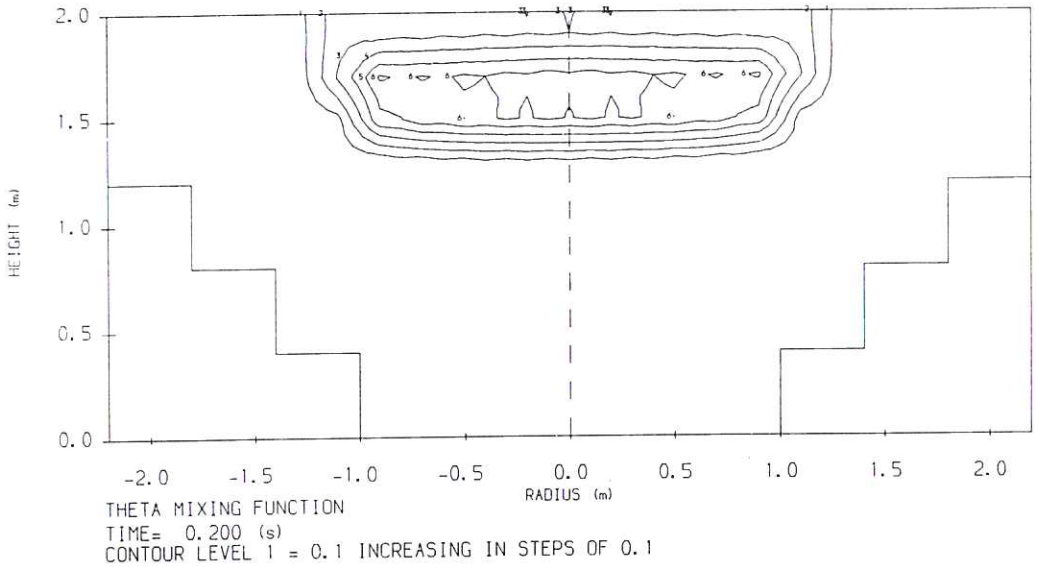

Fig.15(a): Theta function contours at t=0.2s for an ambient pressure of 15MPa.

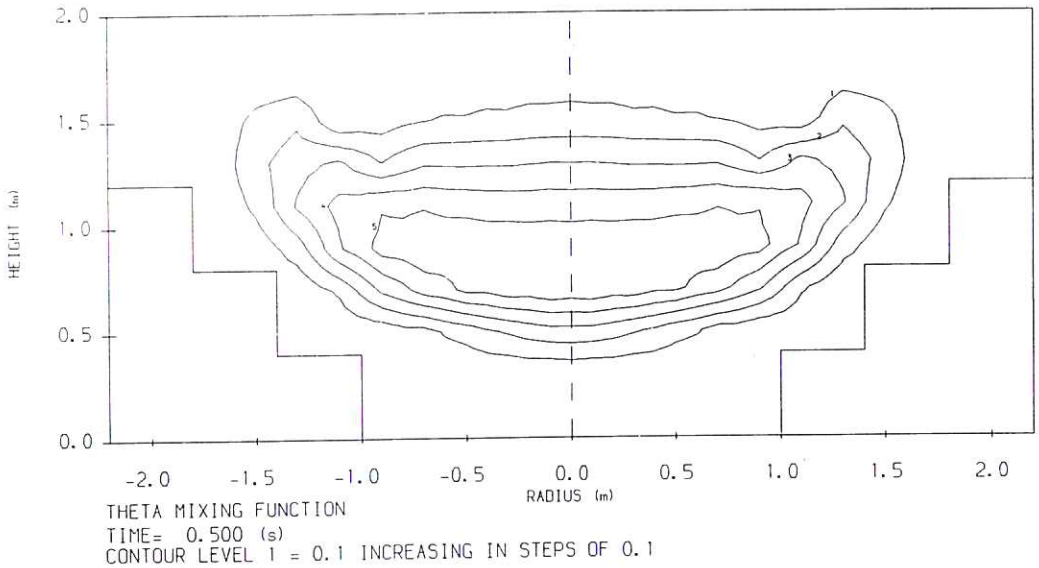

Fig.15(b): Theta function contours at t=0.5s for an ambient pressure of 15MPa.

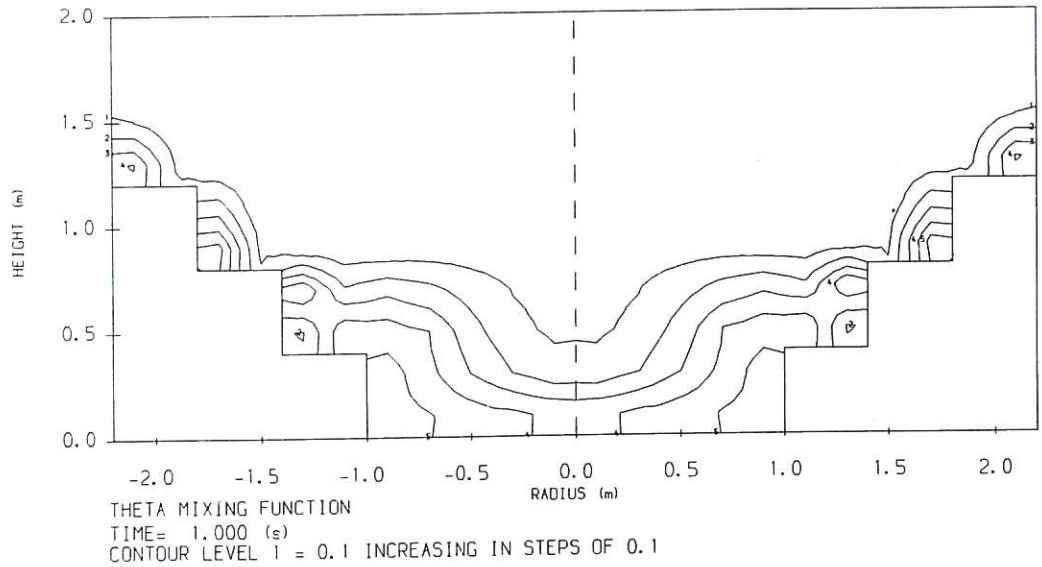

Fig.15(c): Theta function contours at t=1.0s for an ambient pressure of 15MPa.

Available from
HER MAJESTY'S STATIONERY OFFICE
49 High Holborn, London, WC1V 6HB
(Personal callers only)
P. O. Box 276, London, SE1 9NH
(Trade orders by post)
13a Castle Street, Edinburgh, EH2 3AR
41 The Hayes, Cardiff, CF1 1JW
Princess Street, Manchester, M60 8AS
Southey House, Wine Street, Bristol, BS1 2BQ
258 Broad Street, Birmingham, B1 2HE
80 Chichester Street, Belfast, BT1 4JY

PRINTED IN ENGLAND